Journal of Applied Mathematics and Mechanics 73 (2009) 281–289

Contents lists available at ScienceDirect

Journal of Applied Mathematics and Mechanics

journal homepage: www.elsevier.com/locate/jappmathmech

The reflection of a shock wave from a centre or axis of symmetry at adiabatic exponents from 1.2 to 3☆

Kh.F. Valiyev

Moscow, Russia

ARTICLE INFO

Article history:
Received 2 December 2008

ABSTRACT

The self-similar problem of the reflection of a shock wave from a centre or axis of symmetry for adiabatic exponents from 1.2 to 3 with a maximum step of 0.1 is solved. The distributions of the main parameters behind the reflected shock wave are obtained.

The problem of the reflection of a shock wave from a centre or axis of symmetry (henceforth, a centre of symmetry) was solved by Guderley[1] in 1942, and shortly afterwards it was one of the key theoretical elements in developing a thermonuclear weapon, and, at the present time, for controllable inertial thermonuclear fusion. The basis of the solution of this problem is the physically natural assumption of an unlimited increase in the intensity of a shock wave moving towards a centre of symmetry. The second important assumption made by Guderley was that the solution must be self-similar. The self-similarity index, unlike the problem of an intense point explosion,[2] is unknown in advance and must be determined when solving the problem. If the shock wave is intense, then, of the parameters of the gas at rest in front of it, as also in the problem of an intense point explosion,[2] only its initial density ρ_0 is important.

At present, there is only fragmentary information available in the literature on the solution of Guderley's problem. The values of the self-similarity index n, about which we will say more below, were given[3,4] for the spherically and cylindrically symmetrical cases for adiabatic exponents $\gamma = 6/5$, 7/5 and 5/3. Values of the self-similarity index for $\gamma = 6/5$, 7/5, 5/3, 1.87, 2, 2.5, 2.75 and 3 were given in Ref. 5 in the spherically symmetrical case. More information can possibly be obtained in reports (see Ref. 6, where relevant references are given). Of the information available on the parameters behind the reflected jump we have only the values of the density ρ^m behind it for the case of spherical symmetry for two values of γ ($\rho^m = 145$ and 32.7 for $\gamma = 7/5$ and 5/3 (Ref. 3), and $\rho^m = 32.0$ for $\gamma = 5/3$ (Ref. 6)).

Below we obtain a numerical self-similar solution of Guderley's problem in the range $6/5 \le \gamma \le 3$ in steps not exceeding 0.1, and we present detailed information on the parameters behind the reflected shock wave.

1. The self-similar problem of the reflection of a shock wave from a centre or axis of symmetry

A qualitative analysis of the equations. An intense shock wave passes through a cold uncompressed gas at rest to a centre of symmetry. The instant of arrival of the shock wave at the centre of symmetry will be taken as the origin of time t. Then times preceding the arrival of the shock wave at the centre of symmetry will be given values $t < 0$. The distance to the centre of symmetry will be denoted by r. We will seek a self-similar solution of the problem with a self-similarity index unknown in advance, which is determined by the condition for a solution of the problem to exist.[1]

Suppose $\nu = 2$ and $\nu = 3$ in the cylindrical and spherical cases respectively, T is the absolute temperature, s and $h = c_p T$ are the specific entropy and specific enthalpy, c_p is a constant (the specific heat capacity at constant pressure) and v is the gas velocity. After putting $\tau = |t|$ and $u = \operatorname{sign} t$, the equations of the gas motion take the form

$$\frac{d\rho}{d\tau} + \rho\frac{\partial u}{\partial r} + (\nu - 1)\rho\frac{u}{r} = 0, \quad \frac{du}{d\tau} + \frac{1}{\rho}\frac{\partial p}{\partial r} = 0, \quad T\frac{ds}{d\tau} = \frac{dh}{d\tau} - \frac{1}{\rho}\frac{dp}{d\tau} = 0$$
$$\frac{d}{d\tau} = \frac{\partial}{\partial\tau} + u\frac{\partial}{\partial r}, \quad \nu = 2, 3 \qquad (1.1)$$

☆ *Prikl. Mat. Mekh.* Vol. 73, No. 3, pp. 397-407, 2009.

E-mail address: haris_valiev@mail.ru.

0021-8928/$ – see front matter © 2009 Elsevier Ltd. All rights reserved.
doi:10.1016/j.jappmathmech.2009.07.012

We will introduce the required functions, defined as follows:

$$\xi = \frac{r}{K|t|^n} = \frac{r}{K\tau^n}, \quad u = n\frac{r}{\tau}U(\xi), \quad a = n\frac{r}{\tau}A(\xi), \quad p = \rho_0\left(n\frac{r}{\tau}\right)^2 P(\xi)$$
$$\rho = \rho_0 R(\xi), \quad h = \frac{a^2}{\gamma-1} = \frac{1}{\gamma-1}\left(n\frac{r}{\tau}\right)^2 Z(\xi), \quad a^2 = \frac{\gamma p}{\rho} \to Z(\xi) \equiv A^2(\xi) = \gamma\frac{P(\xi)}{R(\xi)} \tag{1.2}$$

Here K is an arbitrary factor. Positive values of u and $U(\xi)$ correspond to the motion of the gas to the centre. The variable ξ takes all values from a certain value ξ_{IS} in the imploding shock wave (IS stands for the imploding shock) up to ∞ on the r axis. Correspondingly, the boundary conditions for the functions R, U and Z must be set for $\xi = \xi_{IS}$.

In the imploding and reflected shock waves (the lines ξ = const) we have

$$\rho_2(u_2 \pm D) = \rho_1(u_1 \pm D), \quad p_2 + \rho_2(u_2 \pm D)^2 = p_1 + \rho_1(u_1 \pm D)^2$$
$$2h_2 + (u_2 \pm D)^2 = 2h_1 + (u_1 \pm D)^2 \tag{1.3}$$

Here and henceforth the upper (lower) sign corresponds to the imploding (reflected) shock wave and D denotes its velocity. The parameters in front of (behind) the shock wave are denoted by the subscript 1 (the subscript 2). Since the trajectory of the shock wave is the line ξ = const, taking formulae (1.2) into account we have the equations

$$D = \frac{dr}{dt} = \mp\frac{dr}{d\tau} = \mp nK\xi\tau^{n-1} = \mp n\frac{r}{\tau}, \quad R_2(U_2 - 1) = R_1(U_1 - 1)$$
$$P_2 + R_2(U_2 - 1)^2 = P_1 + R_1(U_1 - 1)^2, \quad \frac{2}{\gamma-1}Z_2 + (U_2 - 1)^2 = \frac{2}{\gamma-1}Z_1 + (U_1 - 1)^2$$

solving which for U_2 and Z_2 and then substituting $U_1 = 0$ and $Z_1 = 0$ into the expressions obtained, we have

$$U(\xi_{IS}) = \frac{2}{\gamma+1}, \quad Z(\xi_{IS}) = \frac{2\gamma(\gamma-1)}{(\gamma+1)^2}, \quad R(\xi_{IS}) = \frac{\gamma+1}{\gamma-1} \tag{1.4}$$

Expressions (1.2) can be rewritten in the form

$$a^2 = \frac{n^2K^2\xi^2}{|t|^{2(1-n)}}Z(\xi) = \frac{n^2K^2\xi^{2/n}}{r^{2(1-n)/n}}Z(\xi), \quad u = \frac{nK\xi}{|t|^{1-n}}U(\xi) = \frac{nK\xi^{1/n}}{r^{(1-n)/n}}U(\xi) \tag{1.5}$$

On the r axis, where $\xi = \infty$, the values of a and u when $r > 0$ are finite. Consequently,

$$Z(\infty) = U(\infty) = 0 \tag{1.6}$$

After reflection of the shock wave when $r = 0$ and $t > 0$ the pressure p is unlimited, the velocity $u = 0$, and the entropy function p/ρ^γ, conserved in a gas particle, remains the same behind the reflected shock wave, i.e., infinite. For a finite pressure this is only possible when $\rho(0, t > 0) = 0$. By virtue of this, the quantity $T(0, t > 0)$, which is proportional to $p(0, t > 0)/\rho(0, t > 0)$, becomes infinite and $a^2(0, t > 0) = \infty$. By virtue of this and expressions (1.5)

$$Z(0) = \infty, \quad |U(0)| \le \infty \tag{1.7}$$

After substituting representations (1.2) into system (1.1), the equations for determining U, R and Z take the form[2,3]

$$(1-U)\frac{d\ln R}{d\ln\xi} - \frac{dU}{d\ln\xi} = \nu U, \quad (\gamma-1)Z\frac{d\ln R}{d\ln\xi} - \frac{dZ}{d\ln\xi} = \frac{2Z(1/n - U)}{1-U}$$
$$\frac{1}{\gamma}\frac{dZ}{d\ln\xi} - (1-U)\frac{dU}{d\ln\xi} + \frac{Z}{\gamma}\frac{d\ln R}{d\ln\xi} = U(1/n - U) - \frac{2Z}{\gamma} \tag{1.8}$$

The independent variable ξ only occurs in these equations in the form of the differential $d\ln\xi$. Hence, by an appropriate choice of the factor K in the definition of ξ one can put $\xi_{IS} \equiv 1$. The coefficients of the derivatives in Eqs. (1.8) and their right-hand sides do not contain R. The ratio of the derivatives $dZ/d\ln\xi$ and $dU/d\ln\xi$ leads to an equation relating U and Z

$$\frac{dZ}{dU} = \frac{Z}{1-U}\left\{\frac{F(Z,U)}{G(Z,U)}[2/n - (2 + \nu(\gamma-1))U] + \gamma - 1\right\} \tag{1.9}$$

Here

$$F(Z,U) = Z - (1-U)^2$$
$$G(Z,U) = [\nu U - 2(1-n)/(n\gamma)]Z - U(1-U)(1/n - U)$$

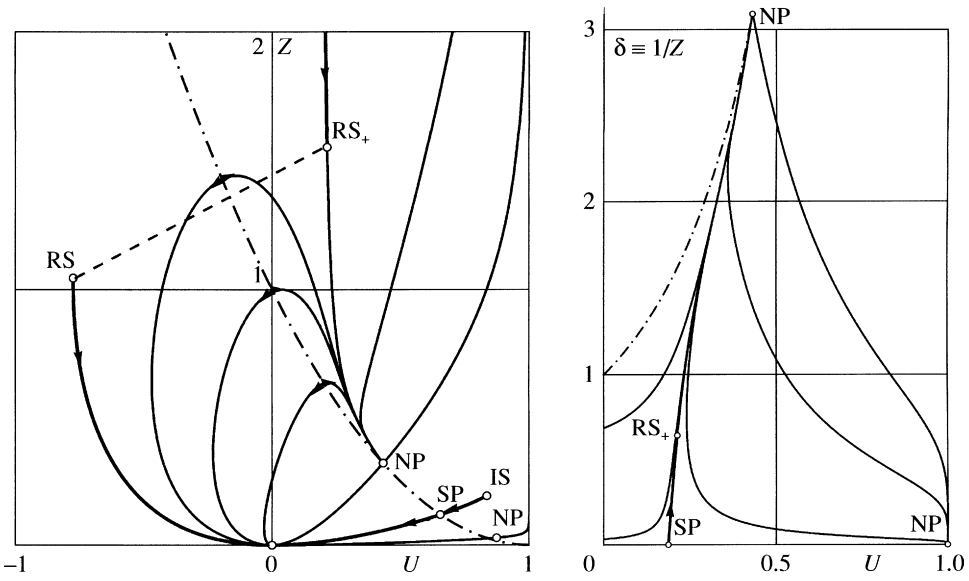

Fig. 1.

The equations for determining ξ and R have the form

$$\frac{d\ln\xi}{dU} = -\frac{F(Z,U)}{G(Z,U)} \tag{1.10}$$

$$(1-U)\frac{d\ln R}{d\ln\xi} = \nu U - \frac{G(Z,U)}{F(Z,U)} \tag{1.11}$$

If the solution $Z=Z(U)$ of Eq. (1.9) is obtained, finding the functions $\xi(U)$ and $R(\xi)$, i.e., the solution of Eqs. (1.10) and (1.11) reduces to quadratures. Hence, the whole problem is primarily reduced to solving Eq. (1.9). The integral curve in the UZ plane emerges from the point IS with coordinates $U(1)$, $Z(1)$ – an image of the imploding shock wave in the UZ plane. The self-similarity index n must be such that the integral curve, emerging from point (1.4), could arrive at the origin of coordinates $Z=U=0$, in accordance with conditions (1.6).

In Fig. 1 we show integral curves for $\nu=3$ and $\gamma=7/5$, and the dash-dot curve is the "acoustic" parabola

$$Z = (U-1)^2 \tag{1.12}$$

On this curve $U+A=1$, or, by the definitions of ξ, U and A from (1.2), $dr/d\tau = u+a$ when $\xi=\text{const}$. Hence, in the rt plane the "singular" C^--characteristic corresponds to the acoustic parabola which, coinciding with the line $\xi=\text{const}$, overtakes the imploding shock wave at the instant of its arrival at the centre of symmetry.

At the point IS

$$Z-(U-1)^2 = (\gamma-1)/(\gamma+1) > 0$$

Consequently, this point lies above the acoustic parabola. As was pointed out above, the required integral curve should arrive at the origin of coordinates, i.e., it must necessarily intersect the acoustic parabola. But according to Eq. (1.10), the derivative $d\xi/dU$ is a fraction with the difference $Z-(U-1)^2$ in the numerator. The monotonic increase in ξ from the value ξ_{IS} on the imploding shock wave up to $\xi=\infty$ on the r axis corresponds to a continuous change in U, including the point where it intersects the acoustic parabola (1.12). According to Eq. (1.10) at its arbitrary points $d\xi/dU=0$. The direction in which ξ increases in Fig. 1 is shown by the arrows. In order that the derivative $d\xi/dU$ at the point of intersection of the integral curve with the acoustic parabola must not change sign, simultaneously with the numerator of the expression for the function $F(Z,U)$ on the right-hand side of Eq. (1.10), the denominator of this expression must vanish, i.e.,

$$G(Z,U) = 0 \tag{1.13}$$

Hence, the point of intersection of the integral curve with parabola (1.5) is a singular point of Eq. (1.9). Equalities (1.12) and (1.13) define its coordinates, while the requirement that the integral curve emerging from it should be incident on the point IS is the self-similarity index n.

An investigation of the singular points of Eq. (1.9) and possible self-similarity indices n was carried out in Ref. 5.

According to the results obtained in Refs 5,6 for values of n of later interest, in general there are two singular points on the acoustic parabola in addition to singular point (1.0). According to Eqs. (1.12) and (1.13) their abscissas are defined as

$$U_{1,2} = \frac{2(1-n)-\gamma(1-\nu n) \pm \sqrt{8n\gamma(n-1)(\nu-1)+[2(n-1)+\gamma(1-\nu n)]^2}}{2n\gamma(\nu-1)} \tag{1.14}$$

If $1<\gamma<\gamma_*$, where $\gamma_*\approx 1.90$ when $\nu=2$ and $\gamma_*\approx 1.87$ when $\nu=3$, the integral curve passes through the lower singular point – a saddle with abscissa U_1, which is obtained when the plus sign is chosen in formula (1.14). This is the point SP in Fig. 1. One of the separatrices

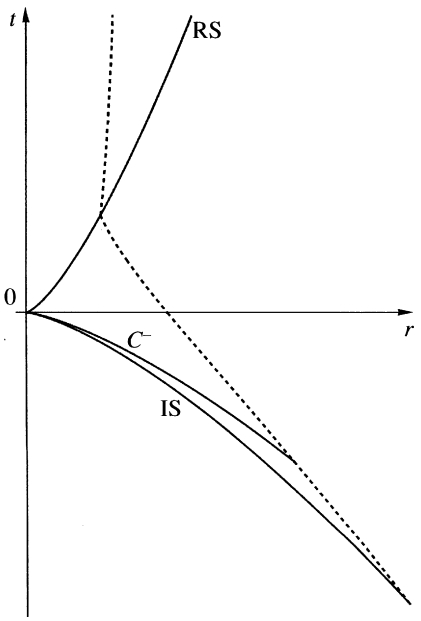

Fig. 2.

passes through the saddle of the integral curve, and the self-similarity index is unique. If $\gamma = \gamma_*$, then $U_1 = U_2$, $Z_1 = Z_2$, and the index n is also unique.

If $\gamma_* < \gamma \le 3$, the integral curve passes through the upper singular point – the node with abscissa U_2. It is obtained when the minus sign is chosen in formula (1.14). We have here considered the case when the integral curve is an isolated branch of the node. In this problem, according to existing results,[5] the separate branch is the unique, integral curve passing through the node with positive slope. Other cases, mentioned in Ref. 5, are not considered.

Hence, for any $1 < \gamma \le 3$ a unique integral curve exists with a positive slope at the singular point, arriving at it from the point IS. After passing through the singular point the integral curve arrives at the origin of coordinates (the point (0,0)) – the node corresponding to the limit values (1.6). In the region of this, Eq. (1.9) takes the form

$$\frac{dZ}{dU} = \frac{2n\gamma Z}{n\gamma U + 2(1-n)Z}$$

Integration of this equation shows that when $U \to 0$

$$Z \approx cU^2 \tag{1.15}$$

Hence, a set of integral curves emerges from the origin of coordinates, which differ by the value of the constant c in formula (1.15).

In Fig. 2 we show, in the rt plane, an imploding shock wave (denoted by IS), the singular C^--characteristic and a reflected shock wave (denoted by RS, standing for reflected shock). They are all lines $\xi = \text{const}$. Moreover, the dashed curve is one of the trajectories of the gas particles.

The shock wave after arrival at the centre of symmetry reflects from it, and, when $t > 0$, expands towards the gas moving to the centre of symmetry. Its expansion law is $r_{RS} = K\xi_{RS}t^n$, naturally, with the previous self-similarity index. As calculations show, behind the reflected shock wave the density reaches its maximum value $\rho^m = \rho_{RS_+}$, and then falls (to zero at the centre of symmetry).

According to formulae (1.7) $Z(0) = \infty$. Hence, to describe the flow between the reflected shock wave and the t axis we must make the change of variable $\delta \equiv 1/Z$. Equations (1.9), (1.10) and (1.11) in U, δ coordinates will be called equations $(1.9)_\delta$, $(1.10)_\delta$ and $(1.11)_\delta$. Equation (1.11) with $\delta = 0$ has two singular points.

The first point is a saddle with coordinates

$$\delta = 0, \quad U = 2\alpha, \quad \alpha \equiv (1-n)/(n\gamma\nu) \tag{1.16}$$

In its neighbourhood, according to Eqs. $(1.9)_\delta$ and $(1.10)_\delta$

$$\frac{d\ln\xi}{d\ln\delta} \approx \beta \to \xi \approx C_\xi \delta^\beta; \quad \beta = \frac{1/2 - \alpha}{1 + (\nu - 2)\alpha}, \quad C_\xi = \text{const} \tag{1.17}$$

As follows from our calculations, the exponent β when $1.2 \le \gamma \le 3$ and $\nu = 2$ and $\nu = 3$ is positive. Consequently, the point (1.16) corresponds to $\xi = 0$, i.e. in this case the flow region reaches the semiaxis $t > 0$. One of the separatrices of the saddle is the straight line $\delta = 0$, i.e. the U axis of the U, δ plane. The second separatrice passes through the upper singular point NP on the acoustic parabola (Fig. 1). Infinite velocity of sound corresponds to the value $\delta = 0$, i.e. $Z = \infty$. In the neighbourhood of the point (1.16) we obtain from Eqs $(1.9)_\delta$ - $(1.11)_\delta$

$$\frac{d\ln R}{d\ln\delta} \approx \Delta \to R \approx C_R \delta^\Delta; \quad \Delta = \frac{\nu}{\nu - 2 + 1/\alpha}, \quad C_R = \text{const} \tag{1.18}$$

The exponent $\Delta > 0$ for all γ and ν. Hence, at the point (1.16), corresponding to the semiaxis $t > 0$, we have $R = 0$ and $\rho = 0$ when $r = 0$ and $t > 0$. When $\delta \to 0$ we obtain from representations (1.2) and formulae (1.17) and (1.18)

$$p = \rho_0 (nr/t)^2 P(\xi) = n^2 t^{2(n-1)} \rho_0 \xi^2 K^2 R/(\gamma\delta) \approx \rho_0 n^2 C_\xi C_R K^2 t^{2(n-1)} \tag{1.19}$$

i.e., the pressure on the semiaxis $t > 0$ is finite and decreases with time.

The second singular point is a node with coordinates

$$\delta = 0, \quad U = 1 \tag{1.20}$$

All integral curves lying above the acoustic parabola to the right of the separatrice of saddle (1.16), emerging from the upper node NP in Fig. 1, enter it. In the neighbourhood of the point (1.20), Eq. $(1.9)_\delta$ takes the form

$$\frac{d\ln U_*}{d\ln\delta} \approx \varepsilon, \quad U_* \equiv 1 - U \to U_* \approx C_U \delta^\varepsilon, \quad \varepsilon = \frac{1}{2\alpha} - 1, \quad C_U \equiv \text{const}$$

Hence from Eq. $(1.10)_\delta$ we also obtain that

$$\frac{d\ln\xi}{d\delta} \approx \frac{C_U \delta^{\varepsilon - 1}}{2\alpha\nu}$$

For all the ν and γ considered, the index $\varepsilon > 2$, and hence as $\delta > 0$ the variable ξ approaches a non-zero value. It can be shown that for $\xi > 0$ the density and pressure vanishes, while the velocity of sound becomes infinite, i.e., a physically non-real flow with the formation of a vacuum cavity corresponds to all integral curves arriving at the node, apart from the horizontal $\delta = 0$. Hence, the flow between the trajectories of the reflected shock wave and the t axis is described by an integral curve arriving at the saddle (1.16).

The transition from the integral curve passing through the node (the point (0,0)) to the separatrice of the saddle (1.16) corresponds to the reflected shock wave, which is described by formulae (1.13). In Fig. 1 RS_- is the point of the integral curve corresponding to the parameters in front of the reflected shock wave, while the point RS_+ corresponds to the parameters behind the reflected shock wave (the arrows on the integral curve indicate the direction in which the variable ξ increases). According to formulae (1.3), U_2 and Z_2 – the parameters on the left of the reflected shock wave – are uniquely defined by the choice of the point on the integral curve 0-RS_-, i.e., the quantities U_1 and Z_1.

By virtue of equalities (1.16) - (1.19) when $\xi \to 0$, i.e., when $r \to 0$, $t > 0$ and the fact that the quantity $\eta = 2\alpha\nu/(2\alpha - 1)$ is negative for all $1.2 \le \gamma \le 3$, it follows that

$$a = C_1 r^{\eta/2} t^{\eta\kappa}, \quad \kappa = n(\gamma - 1)/2 + (n - 1)/\nu, \quad a \to \infty; \quad u = 2\alpha n r/t, \quad u \to 0$$

$$\rho = C_2 r^{-\eta} t^{n\eta}, \quad \rho \to 0, \quad p = C_3 t^{2(n-1)}$$

where C_1, C_2 and C_3 are constants.

2. Features of the numerical solution and results of the calculation

The self-similarity index n was sought in the region in which the above-mentioned singular points exist on the acoustic parabola, and these points must lie in the region $0 < U < 1$, $0 < Z < 1$. Possible values of n must be less than unity and are limited by the condition for the two above-mentioned singular points to exist on the acoustic parabola, i.e., the condition for the radicand in formula (1.14) to be non-negative. Hence,

$$\frac{4 - 6\gamma + 2\gamma\nu + \gamma^2\nu + 2\gamma(\nu - 1)\sqrt{2\gamma}}{(\gamma\nu + 2)^2 - 8\gamma} \le n < 1$$

The index n is defined in such a way that the integral curve, leaving the singular point on the parabola (1.12), arrives at the point IS with the required accuracy. The integral curve in a small neighbourhood of the singular point is replaced by a section of a straight line (call it the straight line A), which is a continuation of the eigenvector of the matrix corresponding to the system of obtained by linearizing a system equivalent to Eq. (1.9) in the neighbourhood of the singular point:

$$\frac{dy}{d\xi} = (y + Z_{1,2}) \times$$

$$\times \left\{ F(y + Z_{1,2}, x + U_{1,2}) \left[\frac{2}{n} - (2 + \nu(\gamma - 1))(x + U_{1,2}) \right] + (\gamma - 1) G(y + Z_{1,2}, x + U_{1,2}) \right\}$$

$$\frac{dx}{d\xi} = (1 - x - U_{1,2}) G(y + Z_{1,2}, x + U_{1,2})$$

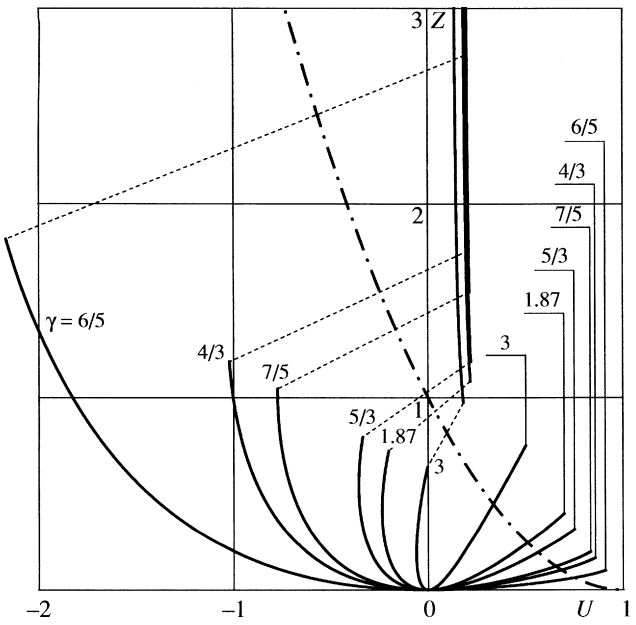

Fig. 3.

Table 1

ν	γ	n	μ	ρ_{IS}	ρ_C	$\rho_{r=0}$	ρ_{RS-}	ρ^m
3	3	0.636411	0.4996	2	2.209	2.736	3.345	4.095
	2.9	0.638365	0.5236	2.053	2.281	2.861	3.539	4.376
	2.8	0.640484	0.5500	2.111	2.360	3.004	3.764	4.707
	2.7	0.642787	0.5792	2.176	2.450	3.168	4.029	5.100
	2.6	0.645300	0.6116	2.250	2.552	3.358	4.343	5.572
	2.5	0.648054	0.6479	2.333	2.669	3.581	4.722	6.150
	2.4	0.651085	0.6887	2.429	2.804	3.845	5.183	6.868
	2.3	0.654437	0.7350	2.538	2.962	4.162	5.758	7.779
	2.2	0.658165	0.7880	2.667	3.148	4.548	6.486	8.961
	2.1	0.662339	0.8491	2.818	3.370	5.026	7.435	10.54
	2	0.667046	0.9207	3	3.641	5.632	8.706	12.72
	1.87	0.674154	1.034	3.299	4.094	6.701	11.14	17.10
	1.8	0.678554	1.108	3.500	4.404	7.470	13.05	20.67
	5/3	0.688377	1.282	4	5.190	9.550	18.88	32.27
	1.5	0.704428	1.600	5	6.814	14.39	36.33	71.72
	7/5	0.717175	1.885	6	8.492	20.07	64.31	145.1
	4/3	0.727686	2.145	7	10.21	26.55	106.9	273.1
	6/5	0.757142	3.016	11	17.33	59.55	539.6	2112
2	3	0.775667	0.5277	2	2.139	2.500	2.991	3.905
	2.9	0.777329	0.5521	2.053	2.203	2.596	3.135	4.144
	2.8	0.779111	0.5788	2.111	2.275	2.704	3.299	4.420
	2.7	0.781028	0.6083	2.176	2.355	2.827	3.488	4.745
	2.6	0.783097	0.6409	2.250	2.447	2.968	3.709	5.131
	2.5	0.785336	0.6773	2.333	2.551	3.132	3.969	5.595
	2.4	0.787769	0.7182	2.429	2.671	3.322	4.281	6.162
	2.3	0.790425	0.7644	2.538	2.810	3.548	4.658	6.867
	2.2	0.793337	0.8171	2.667	2.974	3.817	5.122	7.763
	2.1	0.796548	0.8777	2.818	3.170	4.146	5.707	8.928
	2	0.800112	0.9484	3	3.407	4.553	6.461	10.49
	1.9	0.804099	1.032	3.222	3.700	5.068	7.463	12.67
	1.8	0.808600	1.132	3.500	4.070	5.739	8.844	15.83
	5/3	0.815625	1.302	4	4.749	7.018	11.71	22.98
	1.5	0.826748	1.611	5	6.140	9.818	19.05	44.22
	7/5	0.835323	1.887	6	7.566	12.90	28.77	77.70
	4/3	0.842256	2.138	7	9.018	16.24	41.17	127.5
	6/5	0.861163	2.976	11	15.00	31.62	122.6	590.1

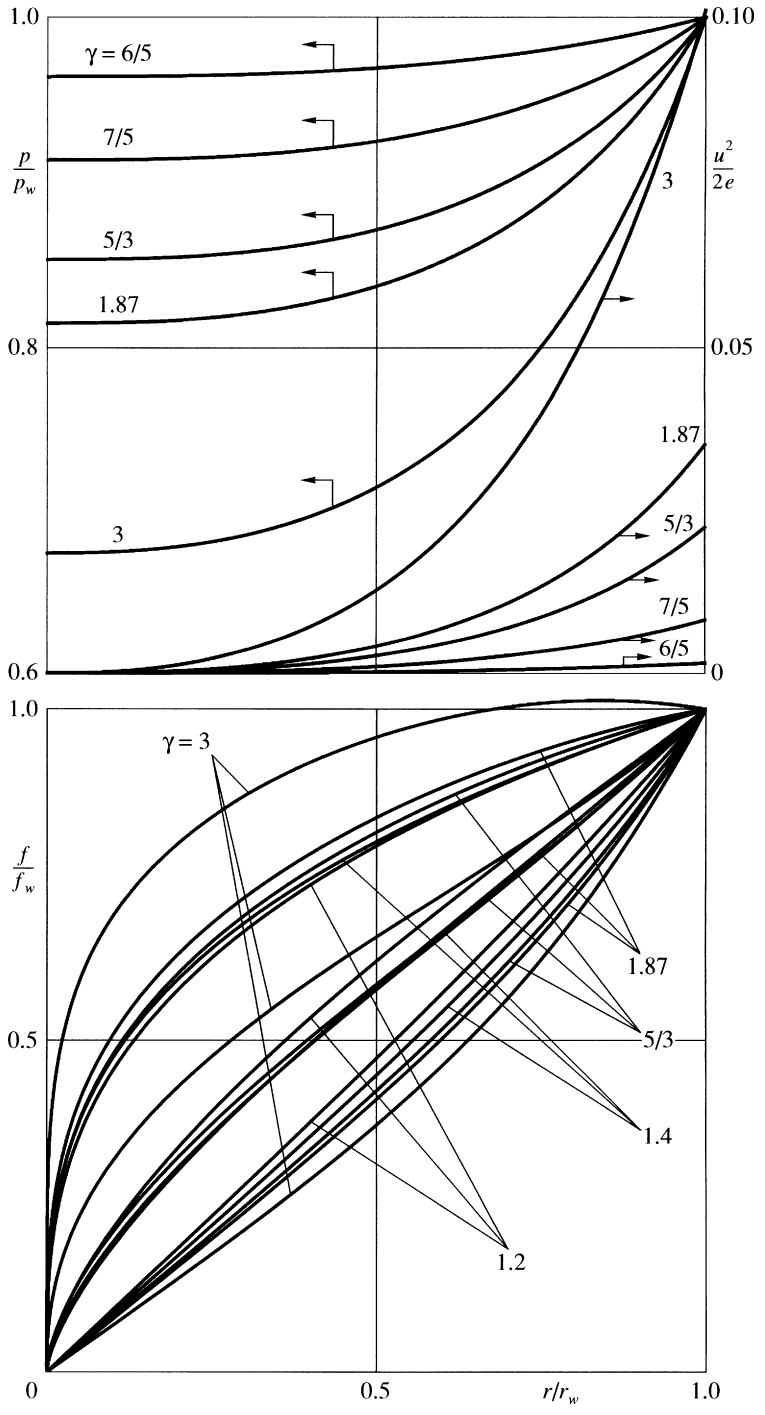

Fig. 4.

Here

$$x = U - U_{1,2}, \quad y = Z - Z_{1,2}$$

and $Z_{1,2} = (1 - U_{1,2})^2$ is the ordinate of the singular point with abscissa $U_{1,2}$ (formula (1.14)). The slope of the straight line A is equal to

$$k = \frac{2k_1}{k_2 + \sqrt{k_3}} > 0$$

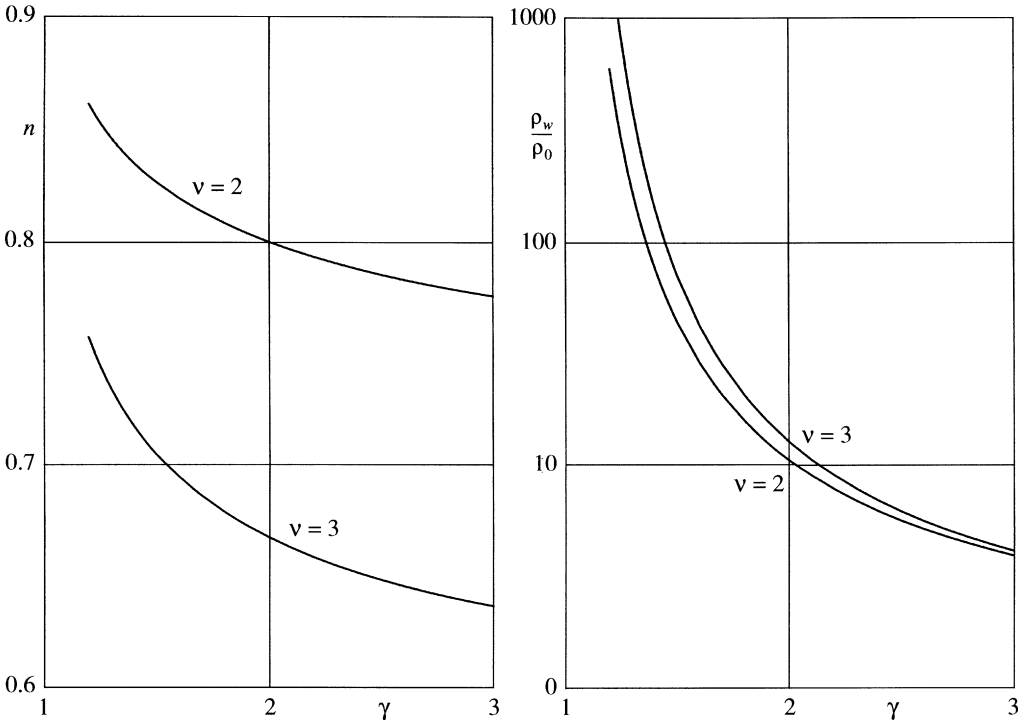

Fig. 5.

where

$$k_1 = (1-U_{1,2})\{5-\gamma+m\nu(\gamma-1)+2U_{1,2}[(m+1)(\gamma-3)-2m\nu(\gamma-1)]+$$
$$+mU_{1,2}^2[7-3\gamma+3\nu(\gamma-1)]\}$$

$$k_2 = 2(m-1)/\gamma+m(\nu-2)-1+2U_{1,2}[3m(3-\nu)+1+(1-m)/\gamma]+mU_{1,2}^2(\nu-5)$$

$$k_3 = k_2^2+4k_1[\nu mU_{1,2}-2(1-m)/\gamma], \quad m = \frac{2+(\gamma-2)U_{1,2}}{2+(\gamma\nu-2)U_{1,2}+\gamma U_{1,2}^2(1-\nu)}$$

After determining the index n, the integral curve of Eq. (1.9), connecting the initial point (1.4) with the point RS_-, is constructed. Transition through the singular point occurs along the straight line A. The second part of the integral curve is obtained by integrating Eq. $(1.9)_\delta$ from the saddle (1.16) to the point RS_+. After the integral curve (more accurately, two of its parts) is drawn in U, Z coordinates, the variables ξ

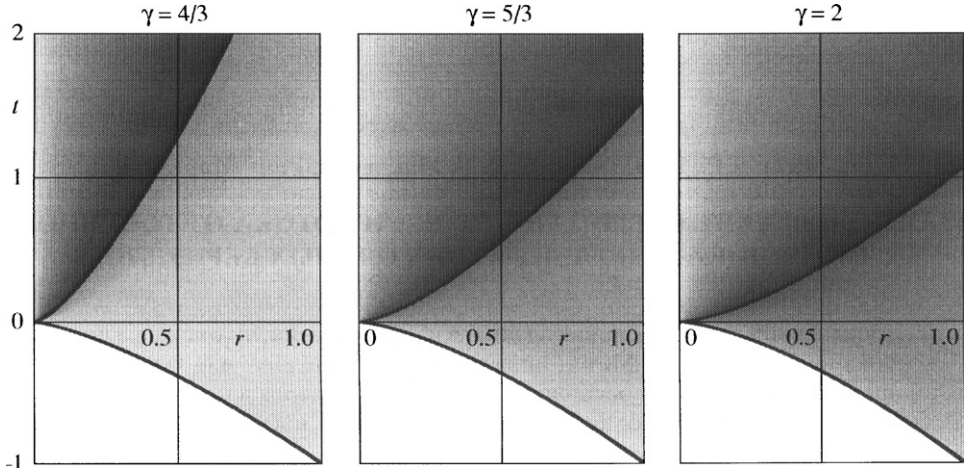

Fig. 6.

and R are found by integrating Eqs (1.10) and (1.11) along it. For $\nu = 2$ and $\nu = 3$ the calculations were carried out for 38 values of γ in the range $6/5 \le \gamma \le 3$. Some of the results are shown in Figs. 3–6 and also in the Table 1. Together with the self-similarity index n the table also shows values of $\mu = U/A$ on the singular C^--characteristic, and also the densities normalized to ρ_0: behind imploding shock wave (ρ_{IS}), on the singular C^--characteristic (ρ_C), and on the r axis ($\rho_{t=0}$), in front of the reflected shock wave ρ_{RS-} and the maximum density behind it (ρ^m). In Fig. 3 we show the integral curve of Eq. (1.9) and the acoustic parabola in the UZ plane for $\nu = 3$ and different γ.

In Figs. 4–6 the subscript w is assigned to parameters immediately behind the reflected shock wave and its coordinate. Figure 4 is drawn for the case $\nu = 3$. In the dependence on r/r_w in its upper part we show the distribution of the pressure p/p_w and the ratio of the kinetic energy of the gas to its internal energy behind the reflected shock wave $u^2/(2e^2)$; in its lower part we show the distribution of the "inverse" velocity of sound a_w/a (the upper family of curves), the density ρ/ρ_w (the middle family of curves) and the velocity of the gas u/u_w (the lower family of curves). In Fig. 5 we show a graph of $\rho^m \equiv \rho_w$ and of the index n against γ for $\nu = 3$ and $\nu = 2$. In Fig. 6, in r, t coordinates, we show the distributions of the density ρ^m for $\nu = 3$ for different values of γ. The coordinates are normalized to the moduli of the coordinates of the initial point of integration on the shock wave, so that at this point $r = 1$ and $t = -1$. The shock waves are shown by the continuous heavy lines. The parts with higher density are darker.

Thus, by a qualitative analysis of the features of the equations of gas dynamics, describing the reflection of a shock wave from a centre or axis of symmetry, we have carried out numerical calculations for the spherically and cylindrically symmetrical cases in the range $1.2 \le \gamma \le 3$ in steps of no more than 0.1. The calculations have shown that the main change in the density, the internal energy and, consequently, the temperature behind the reflected shock wave occurs in a small neighbourhood of the centre or axis of symmetry. Everywhere behind the reflected shock wave the kinetic energy of the gas is a small fraction of its internal energy.

Acknowledgements

I wish to thank A. N. Kraiko for supervising this research.

This research was supported by the Russian Foundation for Basic Research (05-01-00846 and 08-01-00178), in the framework of the Programme for the Support of the Leading Scientific Schools (NSh-9902.2006.1 and NSh-3876.2008.1) and the Analytic Departmental Special Purpose Programme for the Development of the Scientific Potential of Higher Schools (2.1.1/200).

References

1. Guderley G. Strake kugelige und zylindrische Verdichtungsstöße in der Nähe des Kugelmittelpunktes bzw. der Zylinderachse//Luftfartforschung. 1942. Bd 19. Lfg. 9. S. 302-312.
2. Sedov LI. *Similarity and Dimensional Methods in Mechanics*. New York: Academic Press; 1959.
3. Landau LD, Lifshitz EM. *Fluid Dynamics*. Oxford: Pergamon; 1987.
4. Whitham G. *Linear and Nonlinear Waves*. New York: Wiley; 1974.
5. Brushlinskii KV, Kazhdan YaM. Self-similar solutions of some problems of gas dynamics. *Usp Mat Nauk* 1963;**18**(2):3–23.
6. Meyer ter Vehn J., Schalk C. Selfsimilar spherical compression waves in gas dynamics//Zeitschrift für Naturforschung. 1982. Bd 37a. H. 8. S. 955–969.

Translated by R.C.G.